Fluid inclusion and geochemical signatures of the talc deposits in Kanda area, Kumaun, India: implications for genesis of carbonate hosted talc deposits in Lesser Himalaya

Prabha Joshi & Rajesh Sharma

Carbonates and Evaporites

ISSN 0891-2556
Volume 30
Number 2

Carbonates Evaporites (2015)
30:153-166
DOI 10.1007/s13146-014-0196-3

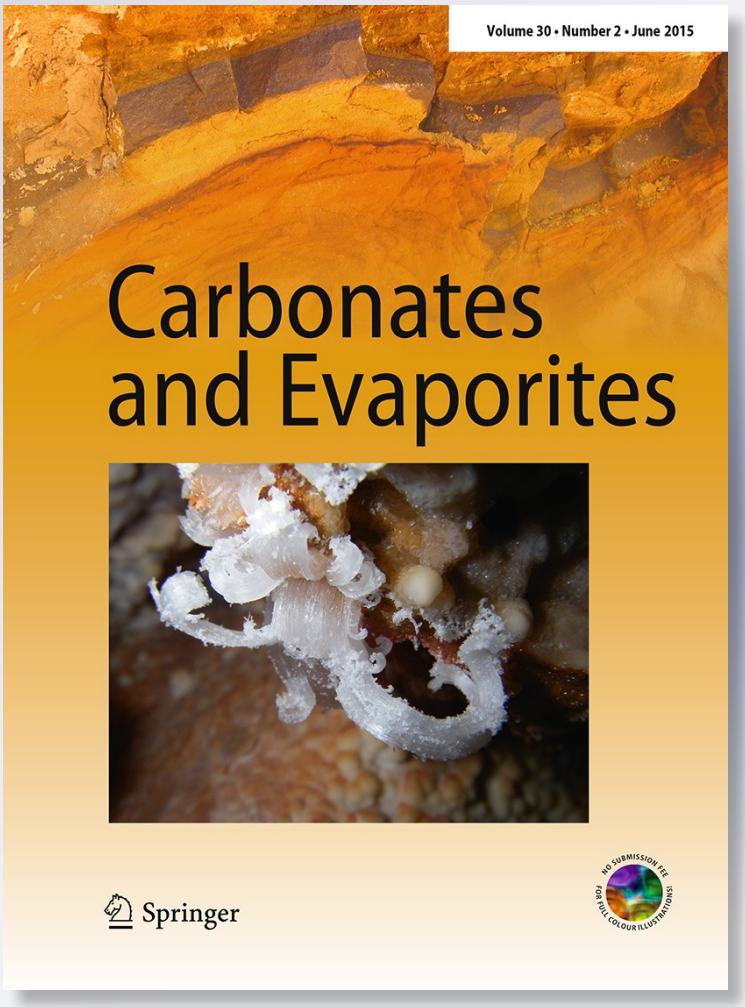

Springer

Carbonates Evaporites (2015) 30:153–166
DOI 10.1007/s13146-014-0196-3

ORIGINAL ARTICLE

Fluid inclusion and geochemical signatures of the talc deposits in Kanda area, Kumaun, India: implications for genesis of carbonate hosted talc deposits in Lesser Himalaya

Prabha Joshi · Rajesh Sharma

Accepted: 28 March 2014 / Published online: 17 June 2014

Abstract Talc deposits in the Deoban Formation of inner Lesser Himalaya in Kumaun are interpreted to have resulted from low-grade, regional burial metamorphism of the siliceous magnesium bearing carbonates consisting of magnesite and dolomite. These deposits are distributed over a large area, occurring in association with magnesite and rarely with dolomite. They are found as fine-grained, fibrous aggregates of talc restricted to small, irregular patches or pockets in carbonate host rocks. Their petrographic features represent different phases of reactions between magnesite and silica to produce talc, thus equilibrium conditions were attained by the assemblage of magnesite + quartz + talc. Scanning electron microscopy also demonstrates that magnesite has reaction margins, whereas dolomite has perfect grain boundary in the magnesite–dolomite–talc assemblage. The major and trace elements in magnesite/dolomite and talc rule out the possibility of any incursion of foreign material during talc formation. Early fluids in magnesite and dolomite were $H_2O + NaCl + KCl \pm MgCl_2 \pm CaCl_2$ in composition, their microthermometry data suggest mixing of the fluids. The fluid inclusion studies also imply that talc was formed under the condition of very low X_{CO_2}. A peak temperature of 300–340 °C and pressure of 2–2.2 kbar are estimated from the coexisting immiscible fluids in talc–magnesite assemblage. It is attributed that the estimated PTX_{CO_2} conditions in the Upper Proterozoic Deoban carbonate rocks, favored the talc formation from magnesite + quartz, and were not conducive to convert siliceous dolomite to talc on a large scale.

Keywords Talc · Magnesite · Fluid inclusions · Lesser Himalaya

P. Joshi
Department of Geology, Kumaun University, Nainital, India
e-mail: prabha_geo@rediffmail.com

Present Address:
P. Joshi
NL-6, Building 5, Flat 2, Bridge View Apartments, Sector 2, Nerul West, Navi Mumbai, India

R. Sharma (✉)
Wadia Institute of Himalayan Geology,
33, General Mahadeo Singh Road, Dehra Dun, India
e-mail: sharmarajesh@wihg.res.in

Introduction

Significant talc deposits are found associated with the platform-type Proterozoic carbonates of the Lesser Himalaya, Kumaun, India. They are wide spread in the Bageshwar District of Kumaun, wherein their pockets and bands are found alternating with magnesite of the Deoban Formation. Kanda talc deposits (29°45′–29°50′N and 79°52′–79°55′E), associated with varying grade and amount of magnesite and dolomite, are representative of these talc deposits of Lesser Himalaya (Fig. 1). The open pit mining is underway for the studied deposits as well as for the other similar deposits that occur in the adjoining parts of the Lesser Himalaya. No evocative study has been conducted on these talc deposits, although considerable attention has been given to the talc mineralization in other parts of the world (Anderson et al. 1990; Dongbok and Lee 2002; Hurai et al. 2011; Kodera and Radvanec 2002; Shin and Lee 2006, etc.). Earlier studies have reported the talc occurrences in parts of the Lesser Himalaya (Gaur et al. 1979; Valdiya 1968, 1980; Sengupta and Yadav 2007). A few of the earlier workers had considered presence of this talc as an evidence for the hydrothermal origin of

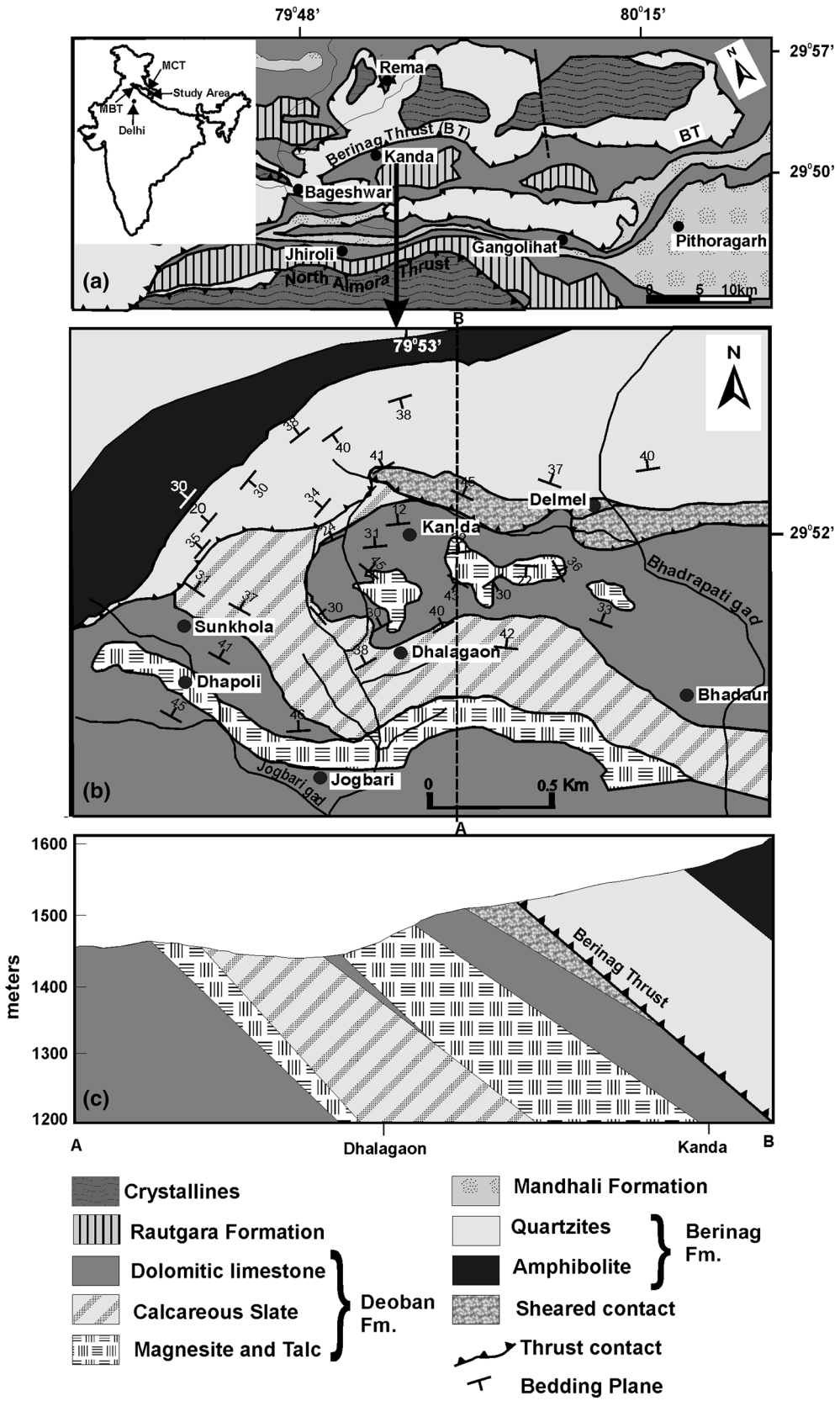

Fig. 1 **a** Regional geological map of Bageshwar and the adjacent area (after Valdiya 1980). **b** Detailed geological map of the Kanda area (after Banerjee and Bisaria 1975). **c** Cross section along A–B line in (**b**)

associated magnesite (Nautiyal 1953; Nath and Wakhaloo 1962). In the present attempt, petrographic, fluid inclusion and geochemical studies are carried out on the talc mineralization and the host rocks from the Kanda area, Kumaun Himalaya, India. These studies delineate the mineralogical characters of talc–magnesite assemblage, reveal fluid conditions during talc formation, and suggest the origin of representative talc deposit from Lesser Himalayan carbonates. This work is significant as a typical case of carbonate hosted talc, and considering the occurrence of similar talc deposits in the Lesser Himalaya on a regional scale.

Geological setting

The Lesser Himalaya, demarcated by the Main Boundary Thrust (MBT) in the south and the Main Central Thrust (MCT) in the north, is a distinct lithotectonic zone of Himalaya. Inner Lesser Himalaya is the northern part of this Lesser Himalaya, lying between the North Almora Thrust in south and the Main Central Thrust in the north (Fig. 1a). A major part of Inner Lesser Himalaya is covered by the sediments of two groups namely Damtha and the Tejam Group. The lower, Damtha Group, comprises flysch and the quartz arenites with basic volcanics, whereas the upper, Tejam Group, consists of carbonate–shale assemblage. These metasedimentary belts include four formations: Rautgara (areno-argillaceous), Deoban (calcareous), Mandhali (phyllitic) and the Berinag Formation (arenaceous). The age of these sediments has been controversial. Initially, on the basis of stromatolites a Riphean age was considered for the carbonates of the Deoban Formation (Misra and Valdiya 1961; Valdiya 1969), but the Vendian age has been assigned to them after the reports of microfossil assemblage from these carbonates (Srivastava and Kumar 1997; Tiwari et al. 2000; Azmi and Paul 2004). On the basis of U–Pb geochronology of the zircons from the crystallines at the base of Berinag Thrust, Celerier et al. (2009) have suggested an age of 1,800–1,880 Ma, and also interpreted that these crystallines are 60 Ma older than the oldest sedimentary rocks of the Inner Lesser Himalaya. They also suggested 800 Ma U–Pb ages for the detrital zircons from the thickly bedded massive sandstone, which lie below the Nagthat Formation in another area of the Lesser Himalaya.

The regional geological set up of the Kanda area has been described by Valdiya (1964), Misra and Banerjee (1968), and Banerjee and Bisaria (1975). The rock formations exposed in the area, are calcareous Deoban Formation and the arenaceous Berinag Formation, which are unmetamorphosed to low-grade, regionally metamorphosed, Proterozoic sediments. Widely present Deoban Formation is autochthonous unit, whereas the overlying Berinag Formation is allochthonous (Fig. 1). The host Deoban Formation occurs on a regional scale, and is characterized by dominant calcareous facies together with subordinate slates. It consists of stromatolitic dolomite, siliceous dolomite, talcose dolomite and dolomitic limestone with intercalations of blue limestone and gray slates (Valdiya 1964). The Deoban Formation also comprises high-grade coarsely crystalline magnesite ± talc, which is widespread in various parts of the Kumaun Himalaya. Valdiya (1980) designated this formation as the Gangolihat Dolomite in the southeastern Kumaun, defining that the Gangolihat Dolomite is the mineralized southeastern facies of the Deoban Formation. The branching and columnar stromatolites are commonly found in the Deoban Formation. Their inversion at the contact of overlying Berinag is because of the southward thrusting of the Berinag Formation. The host rocks in the studied area are sheared, fragmented and at places show crenulations and the kink folds. Axial planes of these folds trend in N–S direction.

The Deoban Formation is overlain by Mandhali Formation that consists of grayish green and black carbonaceous pyritic phyllites and slates with interbedded blue limestone. The contact between Deoban and the Mandhali Formation is perfectly transitional. However, Mandhali Formation is not exposed in the study area because the rocks of Mandhali Formation are overthrusted by the Berinag Formation. Thereby, Berinag Formation is directly resting over the Deoban Formation, completely covering the Mandhali Formation. The Berinag Formation is a huge succession of massive quartzites interbedded with chlorite schists and the amphibolites. These quartzites are moderately to thickly bedded, fine to medium grained and white or yellowish white in color. In western part of the study area, the chlorite schists and amphibolites form a thrust contact with the carbonates of the Deoban Formation.

Talc mineralization

The studied talc is found as steatite confined to the upper part of Deoban Formation. Within this mineralized zone, dolomite and magnesite are crudely interlayered showing enrichment of magnesite in its lower part, while the limestone is not present here. Talc occurs in the form of bands, irregular patches and pockets that are commonly developed within magnesite (Fig. 2a). Talc is schistose to compact massive in nature, and varies in grade because of the impurities of carbonates as seen in the open pit mines of the studied area. Macroscopically talc varies form pure white, dirty white, greenish to grayish varieties depending upon the impurities. Pure talc is white, fine-grained and fibrous, and exhibits pearly luster and soapy feeling, whereas

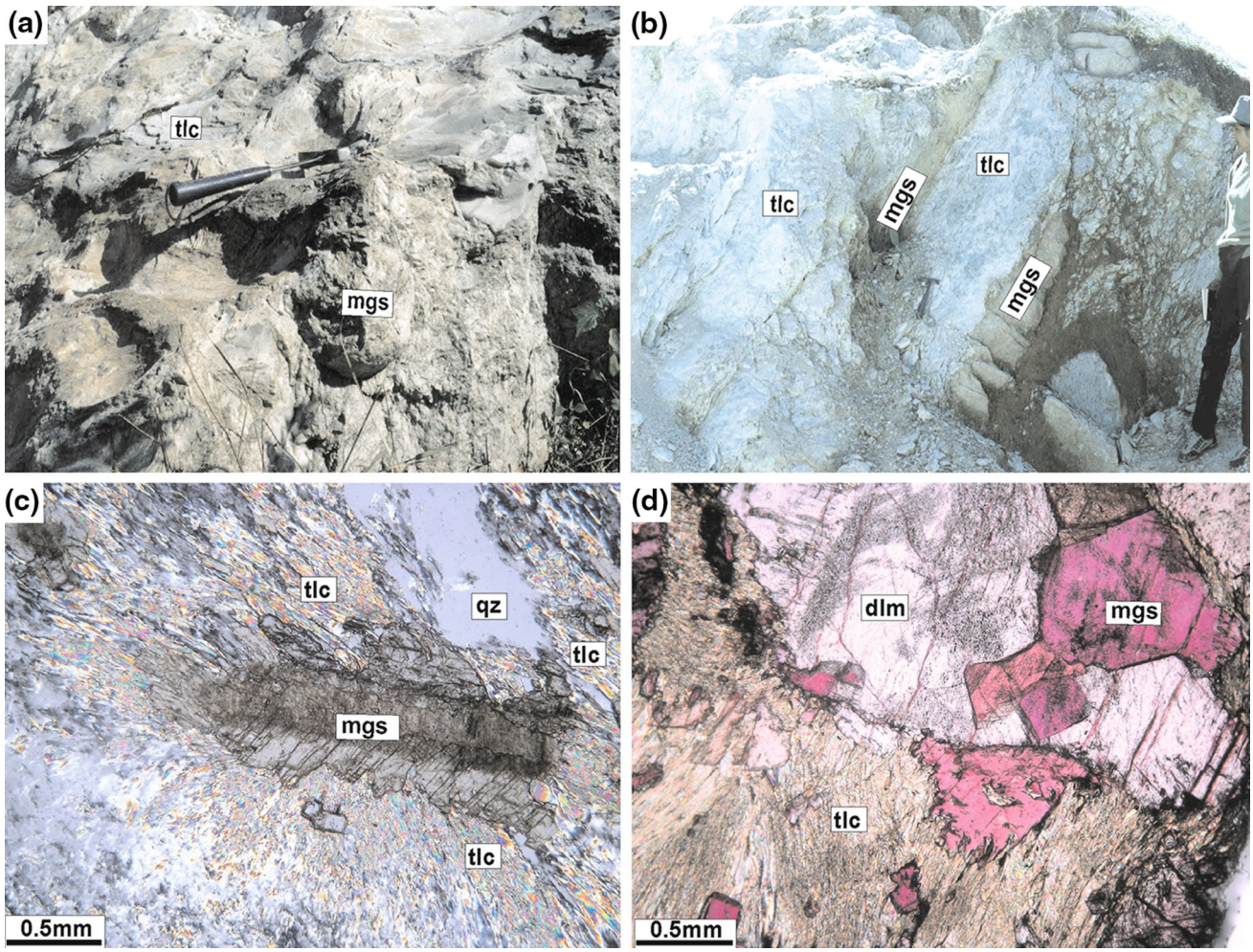

Fig. 2 Field photographs and photomicrographs of the Kanda talc deposit **a** magnesite nodules enveloped by talc layer. **b** Pockets of talc confined in between magnesite bed. **c** Talc developed along the grain boundaries of magnesite. **d** Formation of talc predominantly at the expense of magnesite

impure talc is compact massive and foliated. At times, bands of talc are parallel to the layers of magnesite presenting interlayered relationship. Talc also occurs as vermicular intergrowth and as thin border zone along the magnesite bodies. The contact between talc and magnesite is gradational, but sometimes sharp contact is seen. The magnesite associated with talc is moderately crystalline, white in color, and is characterized by lustrous grains and soapy feeling. Talc-bearing magnesite occurs as pods or lenses within larger dolostone bodies. Thin films and envelops of talc are often developed around stromatolitic and cherty nodules in magnesite (Fig. 2b). The occurrence of talc with dolomite is very limited whereby dolomite together with the developed talc, forms talcose dolomite. Therefore, the talc occurring with dolomite is rather impure. At places, small nodules of dolomite are present within talc bodies. The dolomite associated with talc is gray in color, show a variety of grain size and is fine to moderately crystalline. In addition to these carbonates and quartz, minor siderite and pyrite are observed in impure talc. Siderite mainly imparts reddish to brown color to the talc. The wall rock alteration is absent at the contact of talc and the host rocks.

Petrography

A total 34 number of samples were studied for the petrography observations of magnesite–dolomite–talc–quartz assemblage. Under the microscope, talc is seen varying from very fine-grained aggregates to the well developed flakes of <4 mm size and showing high birefringence. Pure talc occurs as laths exhibiting perfect basal cleavage. Petrographic studies confirm that the talc is predominantly hosted by magnesite but is poorly developed with the dolomite wherein talc flakes are seen as fine-grained fibrous

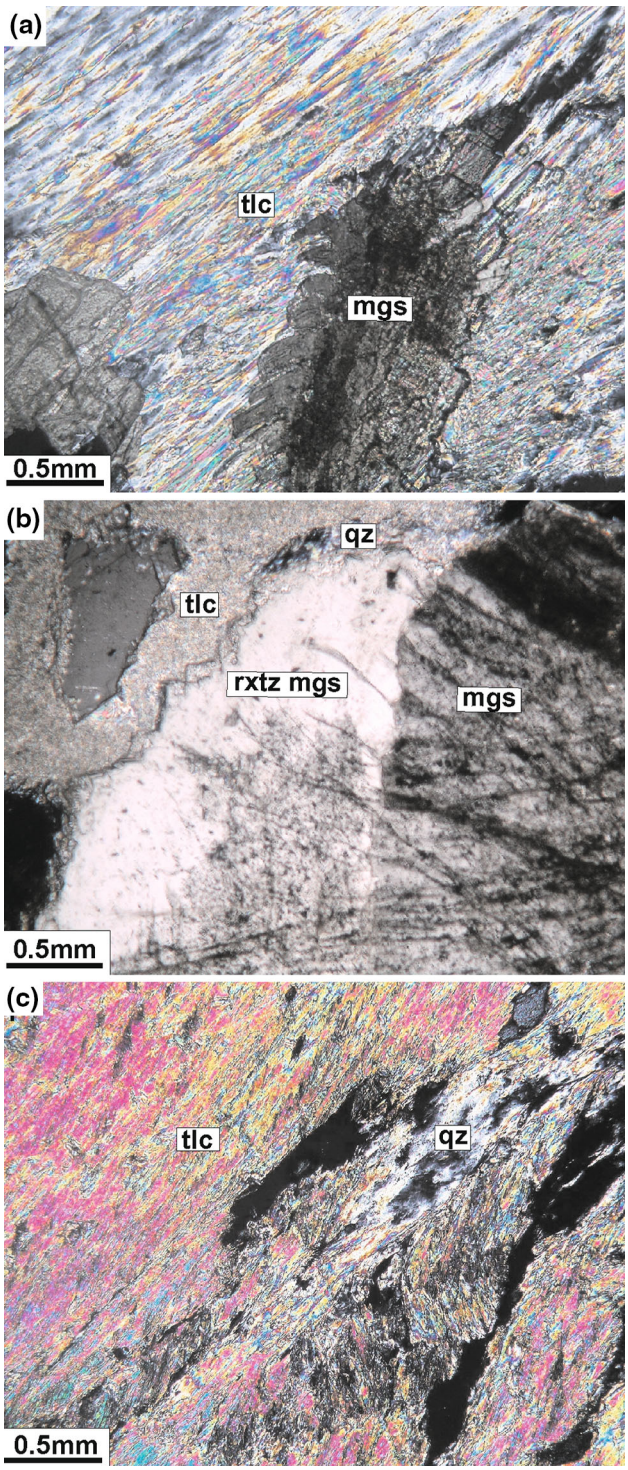

Fig. 3 Photomicrographs showing: **a** magnesite having corroded contact with talc, **b** quartz flakes interleaved with talc and **c** coexisting talc and quartz wherein magnesite has been consumed

aggregates. In association with magnesite, talc is developed along its cleavage and grain boundaries (Fig. 2c, d). The proportion of talc and magnesite is not consistent as evident in number of studied samples. Only magnesite or quartz is found as relict islands encircled by the talc flakes, and such relict grains show corroded boundaries (Fig. 3a). Quartz is present as a primary phase and generally does not occur as late stage veins or infilling of the fractures. Quartz flakes are commonly observed interleaved with talc flakes (Fig. 3b), they are likely originated from the primary cherty layers that were present in the carbonate protolith. An antipathy relationship of talc with quartz + magnesite is noteworthy and such interdependent variation in the proportion of quartz, magnesite and talc has rationale for the conversion of magnesite + quartz into talc, whereby the enriched formation of talc points to the consumption of quartz or magnesite until one is fully consumed (Fig. 3c). The formation of talc at the expense of magnesite is apparent from their common co-occurrence and the grain boundary relations. The evidences such as (1) incipient talc formation along the grain boundaries and cleavage of magnesite, (2) the presence of only magnesite or quartz grains in the talc flakes and (3) their highly corroded boundaries are indicative of the successive stages of talc formation from magnesite + quartz assemblage. Talc is mostly developed with magnesite, and if adjacent dolomite and magnesite is present, it is found encircling the magnesite, whereas, large dolomite grains are left typically un-reacted. The magnesite adjacent to talc is very clear and transparent under the microscope. Although the magnesite and dolomite grains are re-crystallized in the vicinity of talc, but this re-crystallization was not pervasive. As a result, both the re-crystallized grains, i.e. sub-grains showing triple point junctions, and the un-re-crystallized grains are present surrounded by the talc flakes. Numerous euhedral to subhedral, opaque pyrite grains are scattered within the talc flakes and chalcedony fibers. The clinochlore is also found associated with talc. No other silicate phases, except talc, quartz and the clinochlore are present in the mineralized zone.

SEM studies of some of the samples containing different mineral assemblages have been carried out to observe the details of the grain boundaries between various minerals. The representative SEM features (Fig. 4) further substantiate the observations of the thin-section petrography. It is evident that the talc shreds are developed at the contact of magnesite/dolomite, and often magnesite is largely consumed than dolomite thereby un-reacted dolomite and quartz is present (Fig. 4a). Perfect development of talc is seen along the grain boundaries and cleavage of magnesite (Fig. 4b). The initiation of the conversion process of magnesite and quartz is noticed at such planes. Because of this, the margins at their contacts may be corroded (Fig. 4c) at times with penetration of the talc into the magnesite. In the assemblage of magnesite–dolomite–talc, magnesite commonly shows reaction margins whereas dolomite has perfect grain boundaries (Fig. 4d).

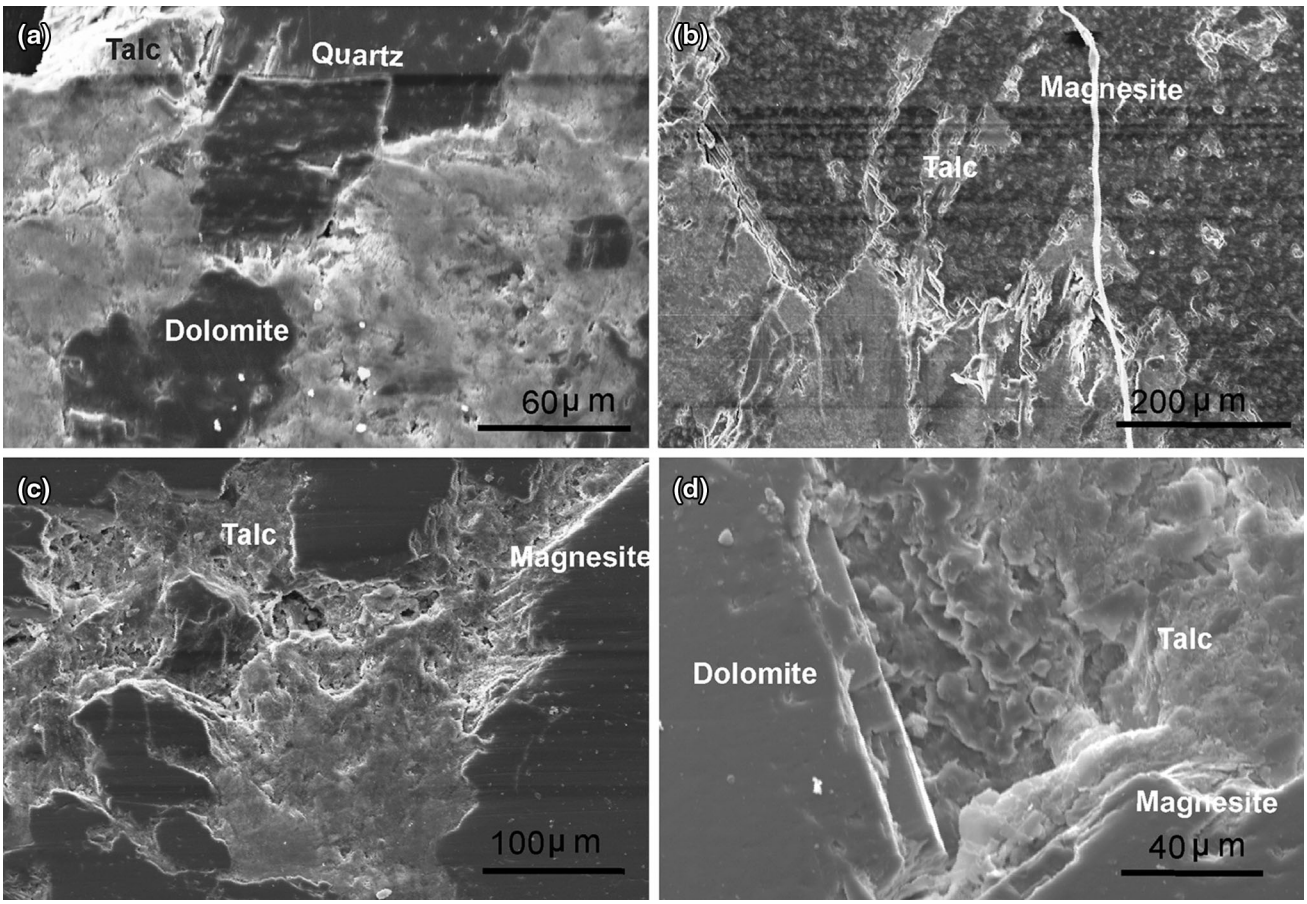

Fig. 4 SEM photomicrographs presenting: **a** un-reacted dolomite and quartz present together with talc. **b** Talc developed along the grain boundaries of magnesite, **c** corroded margins of magnesite and development of talc along such margins, **d** the unreacted dolomite and reacted magnesite together with talc

Geochemical signatures

Samples for major and trace element analyses were selected based on petrography and modal mineral variations. The major and trace element analyses of separated samples of talc, magnesite and dolomite were determined by Wavelength-dispersive X-ray Fluorescence (WD-XRF, Siemens SRS 3000) and ICP-MS (Perkin-Elmer SCIEX) instruments at the Wadia Institute of Himalayan Geology, Dehra Dun. The XRF instrument was calibrated using well characterized international reference samples such as GSR-6 limestone, SDO-1 D-Ohio shale and SGR-1 shale. Analytical accuracy on XRF is better than 5 and 12 % for major oxides and trace elements, respectively, and the precision in terms of observed maximum standard deviation on repeated measurements is better than 2 % (Saini et al. 1998). The relative standard deviation (RSD) for most elements analyzed on ICP-MS is better than 10 %. The data of the analyzed talc samples are given in Table 1, and the representative major and trace elements analyses of dolomite, magnesite and the associated talc are presented in Table 2.

The alterations of dolomite and magnesite to talc are marked by an increase in SiO_2 and decrease in CaO. Marginal increase in MgO content is noticed in talc related to the associated dolomite. Very low CaO in talc indicate that dolomite and calcite are nearly absent within talc. Because Si and Al show an inverse relation and the presence of clinochlore is evident by XRD of talc samples, Al_2O_3 content in pure talc samples from 0.63 to 3.91 is likely because of either presence of clinochlore or replacement of Si by Al in talc layers. Samples showing slightly higher value of Fe_2O_3 may be because of the presence of pyrite, which is present both as fresh grains and altered ones. A very low amount of Sr can be correlated with the low CaO content in talc. The high vanadium content of talc may be due to the higher amount of silica in talc, and is probably derived from the quartz. Vanadium is generally concentrated in the silicate phase and is also very closely linked with trivalent iron because of the crystallo chemical properties of V^{3+} and Fe^{3+}. Because vanadium is an immobile element, it was not leached out in the solution and was concentrated in the talc during its formation. The vanadium does not show any systematic correlation with

Table 1 Major and trace element analysis of talc (results obtained from WD-XRF and ICP-MS)

Sample	P-16	P-17	P-19	P-21	Average
SiO_2	39.62	39.98	42.26	41.07	40.73
Al_2O_3	0.63	3.91	0.92	2.86	2.08
Fe_2O_3	0.33	1.43	0.57	0.82	0.78
MnO	0.00	0.01	0.01	0.01	0.01
MgO	31.28	31.05	31.96	31.60	31.47
CaO	1.67	1.67	2.22	1.65	1.80
Na_2O	0.03	0.08	0.03	0.07	0.05
TiO_2	0.01	0.09	0.01	0.12	0.06
P_2O_5	0.01	0.01	0.19	0.00	0.05
LOI	20.44	16.45	15.35	17.20	17.36
Total	94.02	94.68	93.51	95.39	94.39
Trace elements (ppm)					
Ba	8.3	9.2	7.9	9.4	8.7
Co	0.9	1.1	1.0	1.3	1.1
Ni	2.8	5.9	3.1	4.4	4.1
Pb	21.7	26.2	23.7	26.3	24.5
Sr	2.0	1.8	5.2	1.6	2.7
V	83.5	103.6	97.3	114.2	99.7
Zn	11.7	12.5	9.1	15.1	12.1
Rb	1.4	1.4	1.2	1.2	1.3
U	0.1	0.2	0.3	0.2	0.2
Cu	53	69	60	66	62.0
Cr	3	4	2.5	6	3.9

Table 2 Major and trace element analysis of talc, associated dolomite and magnesite (results obtained from WD-XRF and ICP-MS)

Major oxides	From talc–dolomite association		From talc–magnesite association	
	Dolomite	Talc (P-19)	Magnesite	Talc (P-21)
SiO_2	13.09	42.26	36.16	41.07
Al_2O_3	0.40	0.92	0.99	2.86
Fe_2O_3	2.77	0.57	1.70	0.82
MnO	0.05	0.01	0.03	0.01
MgO	31.73	31.96	34.00	31.60
CaO	12.82	2.22	2.55	1.65
Na_2O	0.02	0.03	0.04	0.07
TiO_2	0.02	0.01	0.02	0.12
P_2O_5	0.01	0.19	0.28	0.00
LOI	45.58	15.35	28.98	17.20
Total	106.49	93.52	104.75	95.40
Trace elements (ppm)				
Ba	16.2	7.9	9.7	9.4
Co	1.7	1.0	1.5	1.3
Ni	5.6	3.1	4.2	4.4
Pb	30.9	23.7	28.4	26.3
Sr	31.1	5.2	5.9	1.6
V	86.4	97.3	89.3	114.2
Zn	25.9	9.1	20.4	15.1
Rb	2.2	1.2	0.7	1.2
U	0.7	0.3	0.7	0.2
Cu	74	60	68	66
Cr	12	2.5	4	6

MgO in talc, and the basic intrusive derived source of higher vanadium and iron is ruled out in view of very low contents of Ni, Cr and Co. Higher Zn in talc may be related to the possibility of minor sphalerite in carbonates, as the presence of sphalerite in the lesser Himalayan carbonates is known from other areas (Sharma 2006; Sharma and Nayak 1991). Most of the major and minor element contents, except the SiO_2, Al_2O_3, Fe_2O_3 and MgO in magnesite and talc, are nearly similar. These elements do not show any significant change and likely point towards sharing of the evolutionary processes between magnesite and talc.

Fluid inclusions study

The fluid inclusion study has been carried out on 18 selected samples of talc–magnesite–dolomite–quartz assemblage to understand 'the fluid and PT conditions' during talc formation. These factors control the formation of talc in the carbonate host rocks. Magnesite, dolomite and quartz in these samples have been attempted for the fluid inclusion microthermometry. The selection of magnesite and quartz for fluid inclusion work is based on: (1) their coexistence with talc, (2) they are likely participants in talc formation, (3) their transparent nature and the availability of workable inclusions, and (4) fluid inclusions are not visible in fine-grained talc. However, the size and the population of inclusions in quartz present crucial limitations. The quartz grains are very small and often do not consist of workable inclusions. Because the petrography indicates talc formation from magnesite + silica, the fluid inclusions data of magnesite has been used over dolomite in the present work. The fluid inclusions are not discernible in talc grains, therefore present work disagree with the earlier contemplation of Sengupta and Yadav (2007) wherein fluid inclusions were studied in talc. Anderson et al. (1990) also opined that fluid inclusions can not be studied in fine talc grains. The microthermometry has been performed at the fluid inclusions laboratory of Wadia Institute of Himalayan Geology, using calibrated LINKAM THMSG 600 stage fitted onto the Nikon E600 microscope. Heating temperatures reported here are correct to ±3 °C and the melting temperatures are precise to ±0.2 to 0.3 °C. Thermometric runs have been repeated on many inclusions to check the leakage and validity of the data. FLINCOR computer program of Brown (1989) has been used to

Table 3 Summarized microthermometry data of aqueous inclusions

Host mineral	Type of the inclusions	Final melting temp. of ice (°C)	Homogenization temp. (°C)	Salinity (wt% NaCl equiv.)	Density (gm/cm^3)
Dolomite	Type I	−1.0 to −7.8	188–237	1.7–11.5	0.87–0. 94
Magnesite	Type I	−5.4 to −12.6	168–267	8.4–16.5	0.86–1.01
Quartz	Type I	−2.1 to −12.5	212–244	3.6–16.4	0.88–0.95
Dolomite	Type II	−3.5 to −9.0	252–288	5.7–12.9	0.81–0.89
Magnesite	Type II	−1.7 to −10.6	172–234	2.9–14.6	0.91–0.98

Table 4 Summarized microthermometry data of aqueous–carbonic inclusions

Host mineral	Temp. of CO_2 melting (°C)	Temp. of CO_2 homogenization (°C)	Temp. of homogenization (°C)	CO_2 density (gm/cm^3)
magnesite	−56.9 to −58.2	+24.5 to +29.8	220–295	0.27–0.71
Quartz	−57.1 to −57.8	+28.3 to 29.8	264–281	0.60–0.65

calculate the density and isochors, whereas table of Bodnar (1993) is used to estimate the salinity of aqueous fluid inclusions. The equation of Zhang and Frantz (1987) has been applied for calculations of aqueous fluid inclusions, and that of Brown and Lamb (1989) for the H_2O–CO_2 inclusions. The inclusions are categorized on the basis of their composition and origin (Roedder 1984; Goldstein and Reynolds 1994). The fluid types observed in different minerals are given below and their microthermometry data are summarized in Tables 3 and 4.

Fluid types in magnesite

Type I: These are primary, biphase aqueous inclusions with liquid phase covering 80–90 volume percent and a complementary vapor bubble. The typical occurrence of these inclusions forming an inclusion rich rhombohedral core (Fig. 5a) and clearer rims in magnesite, strongly favors their primary origin (Goldstein and Reynolds 1994). Inclusions in such distribution are equant in shape, occur within the core of the grains, and show an isolated random distribution (Fig. 5b). Size of these inclusions varies from 5 to 15 μm.

Type II: They are biphase, liquid–vapor aqueous inclusions with liquid covering about 90 volume percent and a vapor bubble. These inclusions are commonly found in clusters and trails, wherein they co-occur with type III aqueous–carbonic inclusions. These are abundant in the recrystallized magnesite grains present adjacent to the talc flakes (Fig. 5c). The part of mineral consisting of these inclusions, is very transparent. Small trails of these inclusions cross-cut the grain boundaries in unrecrystallized magnesite (Fig. 5d), consequently they are considered to be the secondary inclusions in unrecrystallized magnesite. But within the recrystallized magnesite, these inclusions are found in isolated random distribution and at times in growth planes; therefore, they are believed to be trapped during the recrystallisation of magnesite. The shape of these inclusions is equant or tubular. The size of equant inclusions is about 5–10 μm, whereas tubular inclusions vary from 10 to 20 μm.

Type III: These are aqueous–carbonic inclusions, commonly biphase, but in few inclusions a meniscus between aqueous liquid and carbonic liquid is noticed at the room temperature (cf. 21 °C) (Fig. 5c, e). In such inclusions, the bubble of carbonic gas shows Brownian motion within the carbonic liquid. Their carbonic fluid occupies nearly 20–40 volume percent. Type III inclusions occur mostly within magnesite as sub-equant inclusions and as long tubular inclusions of about 10–20 μm size in the planar arrays (Fig. 5f). These inclusions coexist with type II aqueous inclusions (Fig. 5c), pointing to the heterogeneous trapping of the aqueous and carbonic fluids. In a few of them, aqueous fluid is present as a very thin film at the margins of cavity walls forming phase ratio between aqueous and carbonic fluid as about 20:80 or even less and such inclusions appear as monophase.

Microthermometry: Type II H_2O–NaCl inclusions and the coexisting type III aqueous–carbonic inclusions in magnesite are typically abundant adjacent to the talc flakes, and are crucial to the formation of talc. A comparison between the talc bearing and talc-free magnesite and quartz suggest that the aqueous–carbonic fluid is closely associated with talc formation. In view, it is implied that these inclusions are related to the talc formation process. Type I aqueous inclusions are universally present in talc-bearing and talc-free magnesite. It is considered that primary type I inclusions in magnesite are linked to early magnesite mineralization. They are also eliminated if their host magnesite is replaced by talc. Hence, type I inclusions are not significant for the talc formation, therefore are not much discussed here. The initial melting temperatures of type I inclusions widely vary from −45.1 to −24.2 °C. About 90 % of these inclusions show eutectic temperatures

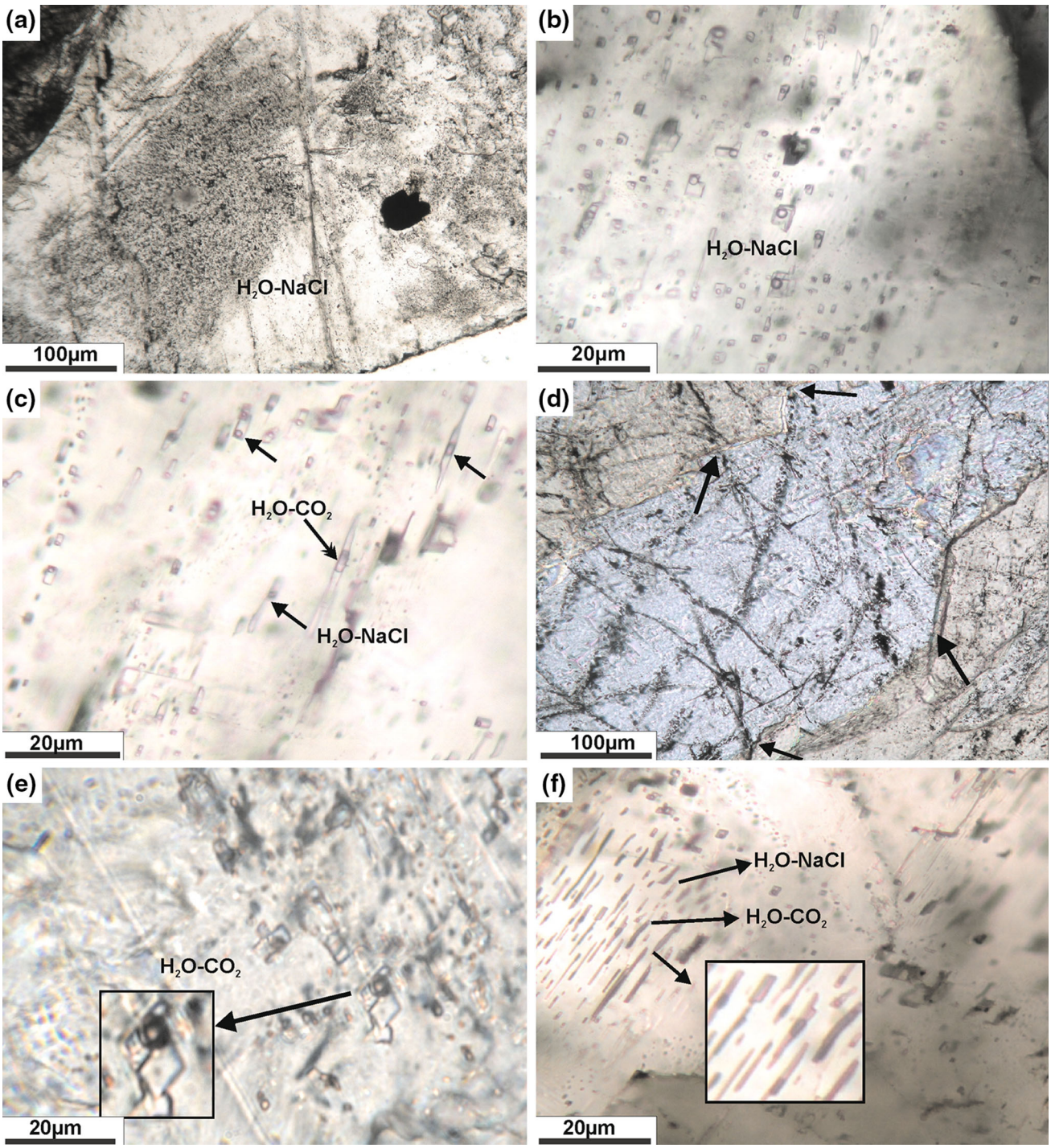

Fig. 5 Photomicrographs of fluid inclusions: **a** inclusion-rich rhombohedral zone with clearer rims in magnesite, **b** primary type I inclusion in magnesite, **c** secondary type II inclusion coexisting with type III in magnesite, **d** type II inclusions in magnesite showing cross cut relation with grain boundary, **e** type III inclusions showing liquid–liquid meniscus (shown by *arrow*). *Inset* shows one such inclusion, **f** type III inclusions as seen in planar array. These inclusions are clear in *Inset*

corresponding to the system $H_2O \pm NaCl \pm KCl \pm MgCl_2$, and the eutectic temperature lower than −35 °C is recorded only in 10 % of these inclusions. The final melting of ice in the frozen inclusions occurred between −5.4 and −12.6 °C. They homogenized to liquid phase at temperatures range of 168–267 °C. Microthermometry of type II H_2O–NaCl inclusions in magnesite is significant in view of their coexistence with H_2O–CO_2 inclusions. Initial melting temperatures of these inclusions vary from −27 to −42 °C, but only three inclusions offered eutectic

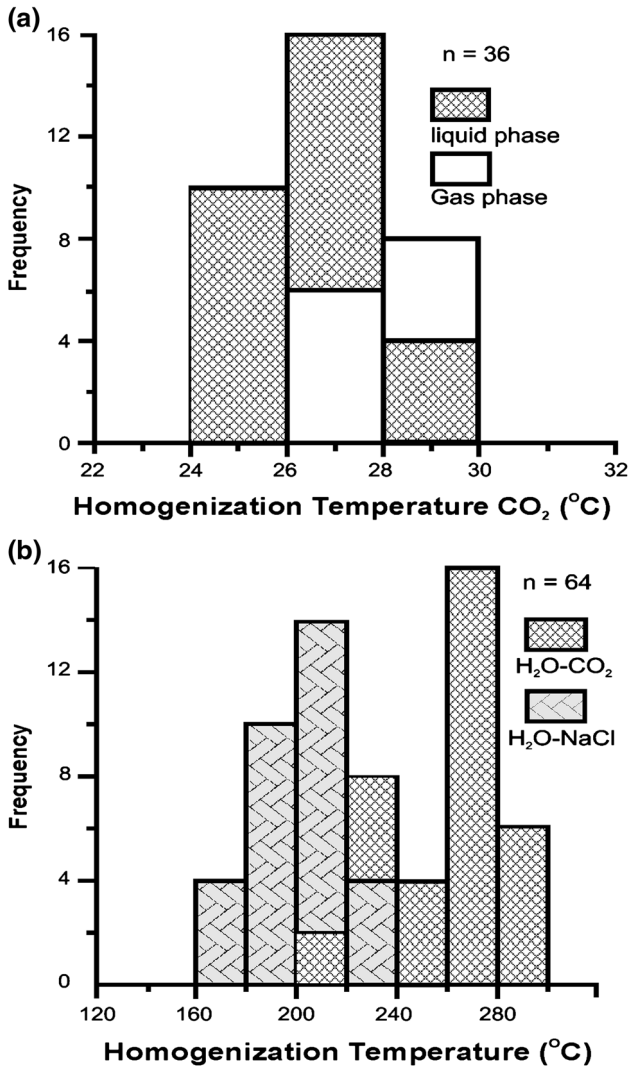

Fig. 6 **a** Histogram of the homogenization temperature of CO_2 phase in type III inclusions in magnesite. **b** Histogram of the total homogenization temperature of types II and III inclusions in magnesite

temperature lower than −35 °C. This suggests predominance of $MgCl_2$ over minor $CaCl_2$ in the H_2O–NaCl ± KCl fluid (Crawford 1981; Bodnar 2003). Their final ice melting temperatures from −1.7 to −10.6 °C correspond to salinity range of 2.9–14.6 wt.% NaCl eq. (Bodnar 1993). These inclusions homogenized to aqueous liquid phase at temperatures varying from 172 to 234 °C, with histogram peak at 200 to 220 °C (Fig. 6b). Frozen carbonic fluid in the aqueous–carbonic inclusions show CO_2 melting within a temperature range of −56.9 to −58.2, implying that this fluid is nearly pure CO_2 and only <8 mol % CH_4 may be present (Heyen et al. 1982). In many of them, CO_2 homogenized to liquid phase at temperatures between +24.5 and +29.8 °C, with peak of the histogram at +26 to +28 °C. However, CO_2 homogenized to the gas phase in some of these inclusions (Fig. 6a). Because of such CO_2 homogenization behavior, their estimated CO_2 densities widely vary between 0.27 and 0.72 g/cm^3. Further, the complete homogenization of aqueous–carbonic inclusions occurred at 220–295 °C, and the peak of the histogram is obtained at 260–280 °C (Fig. 6b). The microthermometry data are summarized in Tables 3 and 4.

Fluid types in dolomite

Type I: Primary, type I inclusions are present in dolomite. These are biphase, aqueous inclusions consisting of >80 volume percent aqueous liquid and <20 percent vapor bubble. They are observed in growth planes and also scattered in the grains, attributing their primary nature. These inclusions are very small, about 2–5 μm in size, and sub-equant to subround in shape. At times, their microthermometry is not possible because of optical limitations.

Type II: Type II inclusions are present in trails, often crosscutting the boundaries of the host mineral grains. In these biphase saline aqueous inclusions, the liquid phase covers about 80–90 volume percent. They are not common in dolomite. Types I and II inclusions differ in their distribution and appearance. Type II inclusions are not as equant as type I, and are also not found in growth planes. These are tubular and sub-regular in shape. The microthermometry data of type I and type II inclusions show little difference.

Microthermometry: The initial melting temperatures of type I inclusions in dolomite range from −21.5 to −28.4 °C, suggesting $H_2O + NaCl \pm KCl \pm MgCl_2$ composition of the fluid. The final melting temperatures of ice in frozen inclusions vary from −1.0 to −7.8 °C, which corresponds to a salinity of 1.7–11.5 wt% NaCl equiv. The salinities of inclusions at histogram peak, vary from 6.45 to 9.21 wt% NaCl equiv. Type I inclusions homogenized to liquid phase at a temperature range of 188–237 °C. The melting of frozen type II inclusions occurred between −3.5 and −9.0 °C, which confirm fluid salinity from 5.7 to 12.9 wt% NaCl equiv. In dolomite, these inclusions homogenized between 252 and 288 °C.

Fluid types in quartz

Type I: Very small two phase aqueous inclusions are present in quartz. The liquid–vapor phase proportion is about 7:3, but this volume estimation may not be precise in 1–3 μm size inclusions. They occur in isolated distribution or in small groups of 3–5 inclusions. Their size is <6 μm, and shape is generally round to sub-round. Uncommon elongated inclusions are also observed. It was not possible to assign primary or secondary origin to these aqueous inclusions.

Type III: Only a few (6–7) aqueous carbonic inclusions are noticed. They are identified in group of the inclusions. The carbonic phase covers about 30 volume percent and an aqueous liquid fills the remaining volume. These inclusions are sub-round to slightly tubular, and their size is <5 μm.

Microthermometry: The initial melting temperatures are recorded in 3–4 inclusions, which vary from −23.2 to −38.5 °C. This is consistent with H_2O + NaCl + KCl ± $MgCl_2$ ± $CaCl_2$ composition of the trapped fluid. Their final ice melting temperatures range from −2.1 to −12.5 °C, analogous to a salinity range of 3.6–16.4 wt% NaCl equiv. They homogenized to liquid phase at temperature range of 212–244 °C. The CO_2 melting in aqueous carbonic inclusions is not clear always, however, it is occasionally seen between −57.1 and −57.8 °C. This CO_2 homogenized to liquid phase at temperatures +28.3 to +29.8 °C, which suggest a CO_2 density from 0.60 to 0.65 g/cm^3. In one inclusion, it is homogenized to gas phase at +26.7 °C (CO_2 density = 0.266 g/cm^3). The total homogenization of aqueous–carbonic inclusions occurred between 264 and 281 °C.

Discussion

The talc deposits are known from a variety of geological environments, but the economically viable deposits are generally found in (1) metamorphosed siliceous Mg-carbonate rocks and (2) altered ultramafic bodies (Brown 1973). The talc deposits associated with ultramafic rocks (Naldret 1966) supply 30 % of the world's talc production. These deposits have their origin from ultramafics and serpentinites, which are chemically near similar to the talc or talc–chlorite mixtures. Alteration of these rocks may result into chemical transfer (Moine et al. 1989) and talc formation. Talc associated with the carbonate host rocks including dolomitic limestone, dolomite, and magnesite constitutes about 70 % of the total talc production. It is known that the formation of such talc requires the availability of silica and magnesium, and the appropriate PTX_{CO_2} conditions. In view, the PTX_{CO_2} for the Kanda talc deposits of Kumaun Himalaya have been evaluated to understand the formation of Lesser Himalayan carbonate hosted talc deposits. Talc, in the area, is confined to magnesite and rarely to the dolomite in the upper part of the Proterozoic Deoban Formation. These talc deposits are stratigraphically restricted in the carbonates of the Deoban Formation, and occur as localized talc pockets and bands along the magnesite, suggesting stratabound nature of the talc mineralization. The volcanics are not noticed within the Deoban Formation, and the quartzites with interbedded basic volcanics of the Berinag Formation was thrusted over the Deoban during tertiary Himalayan orogeny. The evidences, such as the development of talc around stromatolitic and cherty nodules in magnesite, the absence of silicate phases other than talc in the mineralized zone, and the absence of wall rock alteration advocate that an external chemical flux was not responsible for the talc formation. A high temperature hydrothermal activity is ruled out as the wall rock alteration is absent. In the absence of multiphase high-saline fluid inclusions and the large scale carbonic fluid influx such as noticed elsewhere in Poongjeon talc deposits of South Korea (Shin and Lee 2006), diverse origin, mixing and fluid fluxes can not be interpreted for Kanda talc.

The talc–magnesite–dolomite–quartz assemblage of Kanda area show microscopic features, which are helpful in understanding the talc formation. These features are: (1) incipient development of talc encircling the margins of magnesite, (2) defused margins between talc, quartz and magnesite, (3) grains of either quartz or magnesite with highly corroded boundaries are common within the groundmass of talc, (4) the presence of the relict islands of quartz and magnesite in talc, (5) relicts of coexisting magnesite and quartz are rare, and (6) magnesite and quartz showing an antipathy relation with talc. These petrographic features suggest that talc is a product of reaction preferentially between magnesite and silica. As seen in petrography, either silica or magnesite has been consumed at many places of the talc occurrence. Their grain boundaries also characterize their participation in the talc-forming reaction and such features have also been used to comment on the genesis of talc in southwestern Montana (Anderson et al. 1990). The studied talc is commonly developed with magnesite, but poorly developed with dolomite, indicating that the talc formation conditions were not conducive to convert dolomite + quartz into talc. The chemical data favor that Kanda talc was formed from the reaction between the constituents present in the dolomite + magnesite + talc + quartz assemblage, involving a chemical exchange within the system. Most major elements like Mn, Na, Ti, P and the trace elements such as Ba, Ni, Co, Rb, Pb, Cu, U, in dolomite/magnesite and talc are nearly similar. The idea of the formation of Kanda talc from an external chemical flux is not plausible in the absence of any significant abnormal value of elements, such as V, Fe, Ni, Cr and Co that may be indicative of magmatic and/or external source material.

Early fluid in Kanda deposit is represented by the primary type I brine inclusions consisting significant presence of other salts in NaCl aqueous solution. Their ubiquitous presence in magnesite, dolomite and quartz point that the basinal fluids in these Proterozoic calc-magnesian rocks of Lesser Himalaya were H_2O + NaCl + KCl ± $MgCl_2$ ± $CaCl_2$ in composition. In this dolomite–magnesite-bearing assemblage, prevalence of $MgCl_2$ is inferred over $CaCl_2$. It

is interpreted that the salinity up to about 16.5 wt% eq may be because of the longevity of fluid flow and enrichment of Mg in the basinal fluids. The thermal rise up to 267 °C was likely because of the burial and thermal maturation in the basin. A variation in salinity from 1.7 to 16.5 (Table 3) with near-matching salinity at different temperatures, are suggestive of mixing of the fluids. It has been observed that the magnesite and dolomite had undergone some neomorphic changes during late diagenesis, and therefore the subsequent fluids may be related to such events. Because talc is the first mineral that forms during burial metamorphism of the siliceous dolomitic limestone/Mg carbonates, its formation needs to be defined in terms of metamorphic and fluid conditions. The experimental studies as well as the investigations on natural samples suggest that the talc can be formed both from dolomite and magnesite (Winkler 1988; Anderson et al. 1990; Kodera and Radvanec 2002). Talc formation from the magnesite can be represented by the following reaction, which is valid as long as the X_{CO_2} value within the rock is smaller than that of the isobaric point at a given fluid pressure.

$$3MgCO_3 + 4SiO_2 + H_2O = Mg_3Si_4O_{10}(OH)_2 + 3CO_2$$

Abundant aqueous–carbonic fluid inclusions are present in magnesite, typically adjacent to the talc and such occurrence attribute that the trapped CO_2 is a product of decarbonation reaction between magnesite and silica. The location of aqueous–carbonic inclusions in present case implies that the CO_2 fluid was evolved during talc formation. Kodera and Radvanec (2002) also proposed the entrapment of CO_2 fluid by carbonate dissolution during replacement of magnesite by talc, at the Hnusta Mutnik talc–magnesite deposit of Slovakia. The distribution of inclusions in Kanda samples also points that the CO_2-bearing inclusions are younger than type I early brine inclusions and are coeval with type II late brine inclusions. Large scale secondary trails of inclusions and the pervasive fluids flux are not seen. It is suggested that the observed fluids were evolved in the basin as part of within basin fluid system. An open system hydrothermal fluid, such as observed by Hurai et al. (2011), can not be invoked for the Lesser Himalayan talc deposits. Mineralogy suggestive of hydrothermal environment is absent and the fluid phase variations are also not seen.

The PT conditions of the fluid entrapment are significant if the fluids show equilibration with the mineral assemblage. Roedder and Bodnar (1980) demonstrated that the isochors of the coexisting immiscible fluids are vital to calculate the PT conditions in such case. The homogenization temperatures of the coeval aqueous inclusions (type II) and the total homogenization temperatures of aqueous–carbonic inclusions (type III) are <300 °C. Representative isochors of these coexisting H_2O–NaCl and H_2O–CO_2 fluids are plotted to define the PT conditions during talc formation (Fig. 7). These isochors intersects at 2.2 kbar and 340 °C, which are proposed as the PT conditions of talc formation at Kanda. These estimates can be ascribed for the (very) low-grade metamorphism of the Deoban carbonates and for substantial development of talc within these host carbonates.

The formation of talc from the siliceous dolomite through dolomite + quartz + H_2O = talc + calcite + CO_2 need higher PT conditions than those required for the talc formation from the magnesite + silica (Fig. 8). X_{CO_2} of the fluid must be less than 0.1 for the talc formation by reaction of siliceous dolomite (Metz and Puhan 1970; Winter John 2001). Very low X_{CO_2} favors talc formation at low temperatures (Anderson et al. 1990). Further, if the PT is constant and X_{CO_2} exceeds 0.1, talc is not stable and tremolite is formed from the metamorphism of siliceous dolomite. In the CaO–MgO–SiO_2–H_2O–CO_2 system at high temperature, talc is stable within a narrow range although the X_{CO_2} may be widely varying (Tornos and Spiro 2000). Low X_{CO_2} makes talc stable at low temperatures (~300 °C). At very low X_{CO_2}, talc is stable even at supergene conditions (Noack et al. 1986). The homogenization temperatures of aqueous inclusions and the total homogenization temperatures of aqueous–carbonic inclusions are <300 °C. The X_{CO_2} during talc formation can also be calculated considering the phase proportion of CO_2 in the inclusions and its homogenization temperature. The

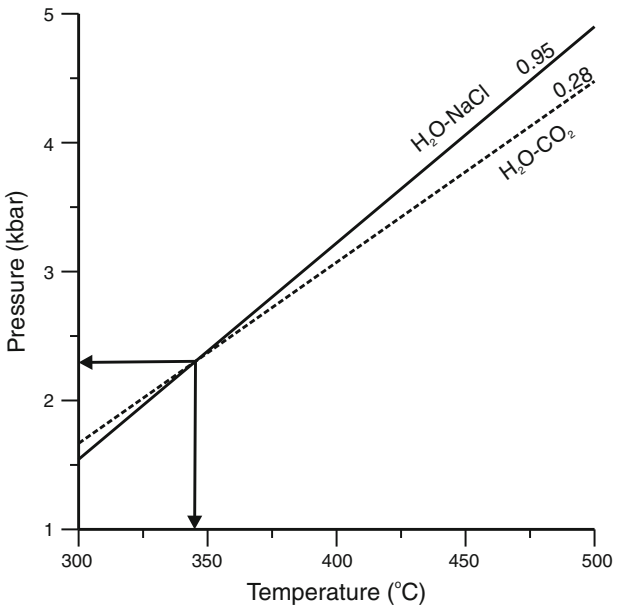

Fig. 7 Representative isochors drawn for the coexisting type II H_2O–NaCl and type III H_2O + CO_2 inclusions. Their intersection suggests P–T conditions of talc formation

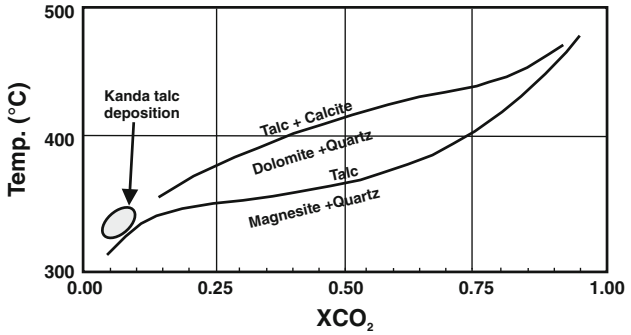

Fig. 8 Isobaric equilibrium curves for talc-forming metamorphic reactions, X_{CO_2} is the mole fraction of CO_2 in the $H_2O + CO_2$ fluid phase. The fluid pressure P_f is 1 kbar (after Winkler 1988). *Stippled area* shows stability field for talc of the Kanda area

fluid calculations using Flincor computer program also provide X_{CO_2}. The X_{CO_2} calculated in present case is low, varying between 0.04 and 0.11. The T-X_{CO_2} diagram at 2 kbar (Shin and Lee 2006) shows that at an X_{CO_2} 0.1 talc is stable at <400 °C. However, at a temperature of about 350 °C, the X_{CO_2} should be too low ($\approx$0.01) for the talc formation from silicious dolomite. Figure 8 shows the isobaric (1 kbar) equilibrium curves with variable partial pressure of CO_2 for the metamorphic reactions: (1) magnesite + quartz = talc and (2) dolomite + quartz = talc + calcite (Metz and Puhan 1970; Winkler 1988). The X_{CO_2} of the fluid must be <0.1 for talc formation form the reaction of siliceous dolomite in regional metamorphism (Winter John 2001). The field of talc formation is proposed using the derived PTX_{CO_2} conditions are also shown in the T-X_{CO_2} field (Fig. 8). In the Kanda talc deposits, the PT conditions were also not adequately high to largely convert dolomite to talc at the derived X_{CO_2}, however, these were favorable to convert magnesite to talc. Herein, the $X_{CO_2} \approx 0.04$–0.1 at a temperature of $\approx$350 °C promoted talc formation at the expense of magnesite instead of dolomite. The abundant talc bodies present in the Deoban carbonates infer that the talc formation process occurred on a regional scale. Hence, it is suggested that the talc deposits in the Deoban carbonates resulted from the favorable PTX_{CO_2} conditions that were attained during the peak burial metamorphism. These conditions promoted talc formation from magnesite over dolomite. One such value: $T = 340$ °C, $P = 2.2$ kbar is derived here for the Kanda talc deposit.

Acknowledgments Authors are thankful to the Director, Wadia Institute of Himalayan Geology, for the encouragement and facilities provided for this work. PJ is thankful to Head, Department of Geology, Kumaun University, for providing the facilities and to Dr. P. D. Pant for encouragement and support. Authors also thank the anonymous reviewers for fruitful suggestions. Council of Scientific and Industrial Research, New Delhi provided financial assistance to PJ in the form of senior research fellowship No. 9/428 (51) 2003-EMR-I.

References

Anderson DL, Mogk DW, Childs JF (1990) Petrogenesis and timing of talc formation in the Ruby range, southwestern Montana. Econ Geol 85:585–600

Azmi RJ, Paul SK (2004) Discovery of Precambrian—Cambrian boundary protoconodonts from the Gangolihat Dolomite of Inner Kumaun Lesser Himalaya: implication on age and correlation. Curr Sci 86(12):1653–1660

Banerjee DM, Bisaria PC (1975) Stratigraphy of the Bageshwar area: a reinterpretation. Himal Geol 5:245–260

Bodnar RJ (1993) Revised equation and table for determining the freezing point depression in H_2O–NaCl solutions. Geochim Csosmochim Acta 57:683–684

Bodnar RJ (2003) Introduction to aqueous-electrolyte fluid inclusions. In: Iain Samson, Alan Anderson, Dan Marshall (eds) Fluid inclusions analysis and interpretation, Mineralogical Association of Canada short course 32:81–100

Brown CE (1973) Talc. US Geol Surv Prof Paper 820:619–626

Brown PE (1989) FLINCOR: a microcomputer program for the reduction and investigation of fluid inclusion data. Am Min 79:1390–1393

Brown PE, Lamb WM (1989) PVT properties of the fluids in the system H_2O–CO_2–NaCl: new graphical presentation and implication of fluid inclusion studies. Geochim Cosmochim Acta 53:1209–1221

Celerier J, Harrison TM, Webb AAG, Yin A (2009) The Kumaun and Garhwal Lesser Himalaya, India: part 1. Structure and stratigraphy. Geol Soc Am Bull 121:1262–1280

Crawford ML (1981) Phase equilibria in aqueous fluid inclusions. In: Hollister LS, Crawford ML (eds) Mineralogical Association of Canada, short course in fluid inclusions: Application to petrology 6:75–100

Dongbok S, Lee IS (2002) The fluid evolution related to Talc mineralization in the Hwanggangri area, South Korea. Resour Geol 52:273–278

Gaur CS, Bagati TN, Nautiyal SP (1979) Magnesite deposits of Bagoli, District Chamoli, Garhwal Himalaya: a preliminary exploration account. Himal Geol 9:744–772

Goldstein RH, Reynolds TJ (1994) Systematics of fluid inclusions in diagenetic minerals. Soc Sediment Geol, Oklahoma, p 199

Heyen G, Ramboz C, Dubessy A (1982) Simulation des-equilibres de phases dan le systeme CO2–CH4 en dessous de 50 C et de 100 bar. Application aux inclusions fluids. C.R. Acad Sci Paris 294:203–206

Hurai V, Huraiova M, Kodera P, Prochaska W, Vozarova A, Dianiska I (2011) Fluid inclusion and stable C–O isotope constraints on the origin of metasomatic magnesite deposits of the Western Carpathians. Slovak Rus Geol Geophys 52(11):1474–1490

Kodera P, Radvanec M (2002) Comparative mineralogical and fluid inclusion study of the Hnusta Mutnik talc–magnesite and Mikova-Jedl'ovec magnesite deposit, Western Carpathians, Slovakia. Bol Parana de Geociencias 50:131–150

Metz P, Puhan D (1970) Experimentelle undersuchung der metamorphose von kieselig dolomitischen sedimenten I. Die gleichgewichtsdaten der reaction 3 dolomit + quartz + H2O = talc + 3 calcite + 3 CO_2 fur die gesamtgasdruckev on 1000, 3000 and 5000 bar. Contrib Mineral Petrol 26:302–314

Misra RC, Banerjee DM (1968) Stratigraphy, correlation and tectonics of Sarju-Pungar valley areas, districts Almora and Pithoragarh, UP. Pub Centre Adv Study Geol Chandigarh 5:101–113

Misra RC, Valdiya KS (1961) The calc zone of Pithoragarh with special reference to the occurrence of stromatolites. J Geol Soc India 2:78–90

Moine B, Fortune JP, Moreau P, Viguier F (1989) Comparative mineralogy, Geochemistry and conditions of formation of two metasomatic talc and chlorite deposits: Trimnous (Pyrenees, France) and Radenwald (Eastern Alps, Austria). Econ Geol 84:1398–1416

Naldret AJ (1966) Talc-carbonate alteration of some serpentinitized ultramafic rocks south of Timmins, Ontario. J Petrol 7:489–499

Nath M, Wakhaloo GL (1962) A note on the magnesite deposits of Almora district, UP. Indian Miner 16:116–123

Nautiyal SP (1953) The reconnaissance geological report of a part of the copper belt Kumaun Himalayas, Almora District, UP. Rec Geol Surv India 89:341–358

Noack Y, Decarreu A, Manceu A (1986) Spectroscopic and oxygen isotopic evidence for low and high temperature origin of talc. Bull Mineralogie 109:253–263

Roedder E (1984) Fluid inclusions, reviews in mineralogy. Miner Soc Am 12:644

Roedder E, Bodnar RJ (1980) Geologic pressure determinations from fluid inclusion studies. Ann Rev Earth Planet Sci 8:263–301

Saini NK, Mukherjee PK, Rathi MS, Khanna PP, Purohit KK (1998) A New geochemical reference sample of granite (DG-H) from Dalhousie, Himachal Himalaya, India. J Geol Soc India 52:603–606

Sengupta HP, Yadav RN (2007) Diagenetic talc of Jhiroli, Kumaun Himalaya. Curr Sci 92:99–103

Sharma R (2006) Nature of fluids and regional implications for Lesser Himalayan carbonates and associated mineralization. J Geochem Expl 89:363–367

Sharma R, Nayak BK (1991) Ore petrology and origin of Pb–Zn deposits in Great Limestone, Riasi, Dist. Udhampur (J&K). J Himal Geol 2:103–110

Shin D, Lee I (2006) Fluid inclusions and their stable isotope geochemistry of the carbonate-hosted talc deposits near the Cretaceous Muamsa Granite, South Korea. Geochem J 40:69–85

Srivastava P, Kumar S (1997) Possible evidences of animal life in Neoproterozoic Deoban microfossil assemblage, Garhwal Lesser Himalaya, Uttar Pradesh. Curr Sci 72:145–149

Tiwari M, Pant CC, Tewari VC (2000) Neoproterozoic sponge spicules and organic walled microfossils from Gangolihat Dolomite, Lesser Himalaya, India. Curr Sci 79(5):651–654

Tornos F, Spiro BF (2000) The Geology and Isotope Geochemistry of the talc deposits of Puebla de Lillo (Cantabrian Zone, Northern Spain). Econ Geol 95:1277–1296

Valdiya KS (1964) A note on the tectonic history and evolution of the Himalaya. Proceedings of the 22nd International Geological Congress New Delhi 11:269–282

Valdiya KS (1968) Origin of the magnesite deposits of southern Pithoragarh, Kumaun Himalaya. Econ Geol 63:924–934

Valdiya KS (1969) Stromatolites of the Lesser Himalayan carbonate formations and the Vindhyans. J Geol Soc India 10:1–25

Valdiya KS (1980) Geology of Kumaun Lesser Himalaya. Wadia Institute of Himalayan Geology, Dehradun, p 291

Winkler HGF (1988) Petrogenesis of metamorphic rocks. Narosa publishing house, New Delhi, p 348

Winter John D (2001) An introduction to igneous and metamorphic petrology. Prentice Hall, New Jersy, p 697

Zhang Y, Frantz JD (1987) Determination of homogenization temperatures and densities of supercritical fluids in the system NaCl–KCl–$CaCl_2$–H_2O using synthetic fluid inclusions. Chem Geol 64:335–350